LBL-12197
Preprint

Lawrence Berkeley Laboratory
UNIVERSITY OF CALIFORNIA

CHEMICAL BIODYNAMICS DIVISION

Submitted to Biopolymers

DNA AND RNA OLIGOMER THERMODYNAMICS: THE EFFECT OF MISMATCHED BASES ON DOUBLE HELIX STABILITY

Jeffrey W. Nelson, Francis H. Martin, and
Ignacio Tinoco, Jr.

January 1981

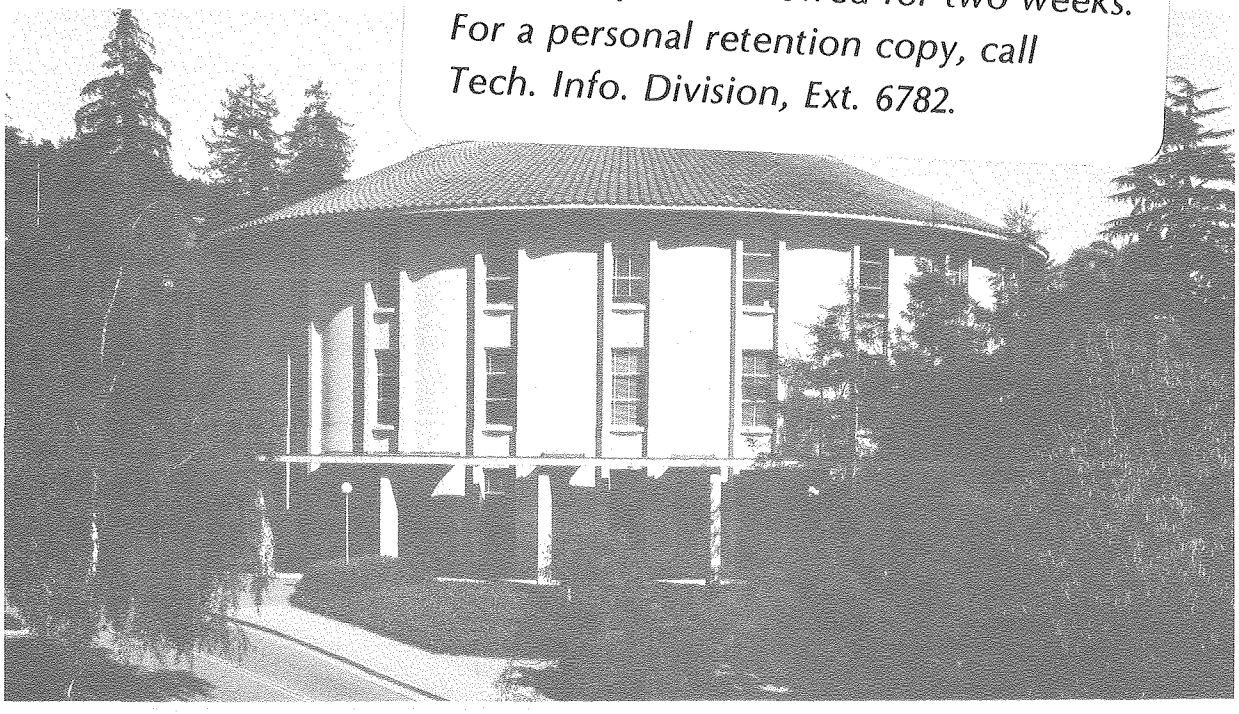

Prepared for the U.S. Department of Energy under Contract W-7405-ENG-48

DISCLAIMER

This work was supported in part by National Institutes of Health Grant GM 10840 and by the Assistant Secretary for Environment, Office of Health and Environmental Research, Biomedical and Environmental Research Division of the U.S. Department of Energy under Contract No. W-7405-ENG-48.

DNA AND RNA OLIGOMER THERMODYNAMICS: THE EFFECT OF MISMATCHED BASES ON DOUBLE HELIX STABILITY

by

Jeffrey W. Nelson

Francis H. Martin

and

Ignacio Tinoco, Jr.

Department of Chemistry

and

Laboratory of Chemical Biodynamics

University of California, Berkeley

Berkeley, California 94720

ABSTRACT

The thermodynamic parameters for the double strand formation of the molecules $rCA_mG + rCU_nG$, m,n = 5-7, and $dCA_mG + dCT_nG$, m,n = 5,6 were measured from optical melting curves. Normal helices are formed when m = n. The deoxy-oligomers are more stable than the ribo-oligomers, due to a more favorable enthalpy. Double helices with mismatched bases can be formed by mixing oligomers with $m \neq n$. Such helices may form several possible structures. A structure with a dangling base is favored over a structure with a bulged base. The destabilization of the double strands by the formation of a bulged base was determined to be greater than 1.6 kcal/mol at 10°C. The extent of aggregation in the oligomer double strand $rCA_7G \cdot rCU_7G$ was determined using ultracentrifugation equilibrium. The possible effects of aggregation on the determination of the thermodynamic parameters for double strand formation are discussed.

INTRODUCTION

Stability of nucleic acid secondary structure is a sequence-dependent property which helps determine the three-dimensional folding of single-stranded DNA and RNA and is likely to affect enzymatic copying of DNA and RNA templates.[1-4] Estimates of stability of RNA secondary structure are usually based on procedures utilizing data obtained from optical melting studies of ribo-oligonucleotides.[5,6] The deoxy-oligonucleotide data base for a similar attempt at DNA stability prediction is more limited.[7-9] Sequence dependence of helix stability is evident from the differences in melting temperature of repeating polymers of identical base composition[10,11] as well as the well-known dependence of T_m on GC content of DNA.[12]

Prediction of secondary structure stabilities have been made taking into account both short and long range interactions. An attempt has been made to predict the high-resolution melting profiles of DNA molecules without taking into account nearest-neighbor (or longer range) effects.[13,14] However, the melting behavior of the duplexes of the block oligomers $d(C_mA_n)\cdot d(T_nG_m)$ have been interpreted as indicating the importance of long range interactions.[8]

The stabilities of perturbed DNA structures might be important in evaluating mechanisms of mutations. In particular, the stability of a bulged base might be important in frameshift mutations by intercalating agents.[15] By chemically modifying a small fraction of adenine bases in poly(A), the destabilizing influence of a bulged modified adenine on the formation of poly(A)·poly(U) was determined to be 2.8 kcal/mol.[16] It should be possible to determine more precisely the nature of this

destabilization by studying oligomer models which lend themselves to more direct physical study.

We have studied the thermal helix-coil transitions of a series of oligomer duplexes of DNA and RNA of related sequence:

$$rCA_mG + rCU_nG;\ m,n = 5\text{-}7$$

$$dCA_mG + dCT_nG;\ m,n = 5\text{-}6$$

These sequences were chosen for study because the terminal G·C base pairs might be expected to minimize fraying of the termini, a complicating factor in previous oligomer studies.[17] Further, these sequences closely model both the frameshift mutational "hotspots" of Streisinger[15] and the sequences of rho-independent transcriptional termination sites.[1,18] We have investigated the possibility that imperfect duplexes of the type rCA_nG + $rCU_{n\pm1}G$ might form bulged double helices such as those which Streisinger has proposed as intermediates in frameshift mutagenesis.[15]

The relative stabilities of DNA, RNA, and DNA·RNA hybrid duplexes of a few of these oligomers have been reported previously and have been related to the process of termination of transcription.[19]

The thermal stability of base-paired complexes can be measured by monitoring any of several physical properties as a function of temperature and oligonucleotide concentration; absorbance of ultraviolet radiation at 260 nm was monitored in the experiments reported here. Proton magnetic resonance studies and calorimetry can give complementary information and have particular advantages, but absorbance methods require less material and allow measurements over a wider range of oligomer concentration. This advantage can become crucial when aggregation may be a complicating factor. Romaniuk et al.[20] have studied the thermal transitions of several ribo-

oligomers including rCAUG using the chemical shifts of nonexchangeable protons at oligomer concentrations on the order of 10^{-2} M. The correlation of these results with those of optical methods at much lower concentrations is problematic without a more complete understanding of aggregation of oligomer duplexes.

The relationship between optical and NMR melting transition measurements are investigated in more detail in a paper[21] reporting the NMR studies on some of the duplexes discussed here.

EXPERIMENTAL METHODS

Deoxy-oligonucleotides were synthesized by the classical diester approach developed in the laboratory of Khorana.[22,23] Reagents employed for blocking of base amino groups were benzoyl (Bz) chloride for adenine, isobutyric (Ib) anhydride for guanine, and anisoyl (An) chloride for cytosine. 5'-hydroxyls were blocked when necessary with the monomethoxytrityl (MT) group, 3'-hydroxyls with acetyl (Ac) groups, and 5'- phosphates with cyanoethyl (CE) groups. 2,4,6-triisopropylbenzenesulfonyl chloride (TPS-Cl) was the activating agent for condensations. Following each condensation, the 3'-hydroxyl blocking group was removed with 1 M KOH in 50% aqueous pyridine (5 minutes at 0°C). Oligomers were synthesized by sequential condensation of dinucleotide or trinucleotide blocks to the 3'-hydroxyl of the growing chain:

$$\underset{(1)}{MTdC^{An}\text{-}OH} + pA^{Bz}pA^{Bz}\text{-}OAc \xrightarrow[2)\ KOH]{1)\ TPS\text{-}Cl} \underset{(2)}{MTdC^{An}pA^{Bz}pA^{Bz}\text{-}OH}$$

$$\underline{1} + \underline{2} \xrightarrow[2)\ KOH]{1)\ TPS\text{-}Cl} MTdC^{An}(pA^{Bz})_4\text{-}OH \qquad (3)$$

$$\underline{3} + pA^{Bz}pG^{Ib}\text{-OAc} \xrightarrow[2)\ KOH]{1)\ TPS\text{-}Cl} MTdC^{An}(pA^{Bz})_5pG^{Ib}\text{-OH}$$

$$\Big\downarrow \text{ deblocking}$$

$$dC(pA)_5pG$$

and similarly for the synthesis of the $dC(pT)_npG$ oligomers. Blocked oligomers were separated by DEAE-cellulose chromatography using triethylammonium bicarbonate (TEAB) and/or ethanol gradients,[24] or by use of reverse phase (C_{18}) columns.[25] Deblocked oligomers were rinsed well at low ionic strength after adsorbance on DEAE-cellulose columns, eluted with a solution of high ionic strength (NaCl or TEAB) and repurified by RPC-5 column chromatography using NaCl gradients at neutral pH. NMR spectra showed no detectable contamination, and all oligomers formed helical complexes specifically with their complements. Ribooligonucleotides were synthesized by enzymatic procedures using primer-dependent polynucleotide phosphorylase (PNPase) at high ionic strength (0.4 - 0.8 M) and appropriate nuclease treatment:

$$rCpA + rADP \xrightarrow{PNPase} rC(pA)_n,\ n = 0,1,2,3,\ldots \text{ (mixture)}$$

$$\xrightarrow{\text{RPC-5 chromatography}} \text{pure } rC(pA)_5 \text{ and other pure } rC(pA)_n\text{'s}$$

$$rC(pA)_5 + rGDP \xrightarrow{PNPase,\ T_1\ RNase} rC(pA)_5pGp \xrightarrow[\text{RPC-5 column}]{\text{alkaline phosphatase;}} rC(pA)_5pG$$

Extinction coefficients of rCA_5G, rCA_8G, rCU_5G and rCU_8G were determined by measurement of absorbance before and after alkaline hydrolysis to nucleotides.[28] Extinction coefficients of other RNA compounds were estimated from the ones measured. Extinction coefficients of the deoxyoligomers were estimated from the extinction coefficients of mononucleotides and dinucleoside phosphates.[29]

Obtaining Melting Curves

The melting curves were measured on a Gilford Model 250 spectrophotometer equipped with a Gilford Model 2527 thermoelectric temperature programmer. The data were collected either by recording the absorbances and temperatures manually, or automatically by a Commodore PET Model 2001 microcomputer via an interface to the Gilford spectrophotometer. The readings were at 260 nm, with a temperature scan rate of 1°C/min. At this rate, the instrument exhibited no lag between the temperature in the cell and that indicated by the thermo-programmer.

The cells for the Gilford have dimensions of 1.2(ℓ) x 0.6 (w) x 1.9(h) cm. The pathlengths were 1.0, 0.5, 0.2, or 0.1 cm. Pathlengths of 0.01 and 0.02 cm were obtained by using a 0.2 cm cell fitted with a quartz spacer of 0.19 or 0.18 cm, respectively. The actual pathlengths were determined from absorbances of sodium dichromate solutions of known concentrations. The pathlengths of 0.1 cm and longer were essentially correct; those of the 0.01 and 0.02 cm varied somewhat between different cells and spacers. The pathlengths of all the combinations were determined.

Evaporation was controlled in cells without stoppers by floating silicon oil (Dow Corning 200 Fluid, 20 cs viscosity) over the sample. This had no effect on the absorbance of the solution, and was very effec-

tive in reducing evaporation. In cells with teflon stoppers, no oil was used. In most cases, the samples were returned to 0°C after the melting curve was completed. The evaporation, as indicated by an increase in absorbance, was usually less than 1%. Samples with evaporation greater than this were not used in the analysis.

The cells were soaked in concentrated nitric acid before using. The samples were degassed either by purging the buffer with helium prior to mixing, or by heating the samples briefly to about 60°C and shaking to eliminate bubbles prior to filling the cells. The buffers used were either 0.2 or 1.0 M NaCl in 0.01 M phosphate buffer, pH 7, and 0.1 mM EDTA.

Analysis of Melting Curves

The thermodynamic parameters were obtained from melting curves using the method of Martin et al.[26] We plot the relative absorbance versus temperature by normalizing the absorbance of single strands to 1.0 at 50°C. This allows us to directly compare the melting at different concentrations. In some cases, the double strand to single strand transition is not complete at 50°C. In these cases, the absorbance of the single strands at 50°C is obtained by extrapolating from higher temperatures (see Figure 1).

If we know the upper (single strand) and lower (double strand) baselines, we can determine f, the fraction of strands in double helices at any temperature, from the formula:

$$1 - f = \frac{A(T) - A_d(T)}{A_s(T) - A_d(T)} \qquad (1)$$

where $A(T)$, $A_d(T)$, and $A_s(T)$ are the relative absorbances of the experimental curve, the lower baseline, and the upper baseline, respectively. Since the oligomers in this study are not self-complementary, we can directly measure $A_s(T)$, the single strand baseline. However, $A_d(T)$, the double

strand baseline, can only be estimated from the behavior of the melting curve at low temperatures.

We can relate f to the equilibrium constant using Equation (3) by setting $C_a = C_b$, the total concentrations of oligomers A and B, respectively:

$$A + B \rightleftarrows DS$$

$$f = \frac{(DS)}{(DS) + (A)} = (DS)/C_a \tag{2}$$

$$K = \frac{(DS)}{(A)(B)} = \frac{f}{(1-f)^2 C_a} \tag{3}$$

We define the melting temperature, T_m, as the temperature at which half of the strands are in double strands (f = 0.5). From the concentration dependence of the T_m, we can calculate the $\Delta H°$ for the transition from the slope of a plot of $1/T_m$ vs. the log of the concentration:

$$\Delta H° = 2.303R \frac{d \log(C_a)}{d(1/T_m)} \tag{4}$$

where C_a is the total concentration of each of the oligomer strands.

In addition, assuming a two-state model, we can determine $\Delta H°$ from the slope of a melting curve at the T_m, using the formula:

$$\Delta H° = 6 R (T_m)^2 (df/dT)_{T_m} \tag{5}$$

The $\Delta H°$ calculated by both equations should agree if the system is two state, and we have drawn the baselines correctly.

Equilibrium Ultracentrifugation

Equilibrium ultracentrifuge experiments were carried out on the single strand rA_7G, and the double strands formed from rCA_7G + rCU_7G, using a Beckman Model E analytical ultracentrifuge equipped with ultraviolet scanning optics. The speed was controlled and monitored electronically.

For rA_7G, a sample with a concentration of 180 μM was prepared in a 1 M NaCl solution, using a centrifuge cell with a 1 mm double sector titanium center piece. The centrifuge was run at 34,900 rpm (3660 rad/sec) at a temperature of 2°C. Scans were taken several hours apart until successive scans were the same, indicating that equilibrium had been attained. The total time of the experiment was four and a half days. The absorbance at 260 nm was too high to measure, therefore, scans were taken at 265, 270, 275, 280 and 285 nm. The final concentrations ranged from 18 μM at the top of the cell to 490 μM at the bottom.

The double strand experiment was performed using the same 1 mm cell, using an initial concentration of 220 μM in both rCA_7G and rCU_7G. A speed of 20,400 rpm was used (2140 rad/sec); the temperature was controlled at 3°C. The attainment of equilibrium was determined in the same manner as above. The final concentrations were 27 μM at the top and 1200 μM at the bottom. The equilibrium constant at 3°C for rCA_7G + rCU_7G double strand formation is 1.0×10^9, so at a concentration of 27 μM, greater than 99% of the strands are in double helices. The scans were taken at 280, 285, 290 and 295 nm. The total time of the experiment was again four and a half days.

RESULTS

The melting curves for seven concentrations of $dCA_5G + dCT_5G$ in 1 M NaCl are shown in Figure 1. The curves are all normalized to an absorbance of 1.0 at 50°C. The upper line is the experimental melting curve for the single strands. The melting curves do not superimpose at low temperatures; the hypochromicity increases with higher concentrations. This effect is due to aggregation of the double strands, and will be discussed later. Because of the concentration dependent hypochromicities, we assign a different baseline to each curve, depending on its individual hypochromicity. If one baseline is chosen for all of the curves, the results are significantly different.

The melting curves do not have zero slope at low temperatures. This effect could be due to a temperature dependent extinction coefficient due to a small conformational change, or perhaps differential melting of the ends. We did the analyses using both flat and sloping lower baselines. The resulting hypochromicities and melting temperatures (T_m) for each concentration are shown in Table 1 for $dCA_5G + dCT_5G$. We can determine $\Delta H°$ from a plot of $1/T_m$ vs. log (C_a) using Equation (4). The resulting plots are essentially straight lines, as shown in Figure 2.

Table II summarizes the results of the analyses, including the $\Delta H°$ calculated from the slope of the melting curve using Equation (5). In addition to $\Delta H°$, $\Delta S°$ and $\Delta G°$, we tabulate the T_m for a solution 200 μM in each strand (400 μM total strand concentration) as a reference to compare stabilities of different oligomers. This corresponds to a concentration of 100 μM for a self-complementary oligomer. The $\Delta H°$ calculated from the concentration dependence is essentially the same, whether flat

or sloping baselines are used. However, the value for $\Delta H°$ calculated from the slope of the curve at the T_m using Equation (5) increases when using a sloping baseline. The stability, as indicated by the $\Delta G°$ or the T_m (200 μM) increases when a sloping baseline is used. This is simply because the T_m's are shifted to higher temperatures. We will use flat baselines unless specifically noted. This will allow us to make direct comparisons to earlier work, all of which assumed flat lower baselines. We will also use values for $\Delta H°$ derived from the concentration dependence of the T_m.

Table III compares the thermodynamics of $dCA_5G + dCT_5G$ with $rCA_5G + rCU_5G$, in 0.2 and 1.0 M NaCl. The $\Delta H°$ for the deoxy-oligomers is about 7-8 kcal greater than for the ribo-oligomers. In both cases, the $\Delta H°$ does not change significantly when the salt concentration is increase from 0.2 to 1.0 M NaCl, although the stabilities increase somewhat, 2.4°C for the deoxy-, and 4.7°C for the ribo-oligomers.

The effect of chainlength on the thermodynamic stability of ribo-oligomers are tabulated in Table IV for the oligomers $rCA_nG + rCU_nG$, where n = 5 to 7, in 1.0 M NaCl. The values calculated using the parameters from Borer et al.[6] are shown below the experimental parameters. The calculated stabilities are lower than those observed experimentally, although the agreement is better for the longer oligomers. It is also seen in Table IV that the values for $\Delta H°$ calculated from the concentration dependence of T_m and from the slope of the melting curve at the T_m agree fairly well for $rCA_5G + rCU_5G$ and rCA_6G and rCU_6G, but differ significantly for $rCA_7G + rCU_7G$.

When oligomers are mixed with unequal numbers of A's and U's (or T's), the double helices can form bulged structures. One example is mixing

rCA_6G with rCU_5G. The results of such mismatches are shown in Table V. The mixtures rCA_7 + rCU_5G and rCA_5G + rCU_7 are included to compare the "bulged" structure to a helix which must dangle bases off one end. The thermodynamics for the normal double helices are included for comparison. Since the mismatched double strands are not stable at 25°C, the values for $\Delta G°$ are tabulated at 10°C. The "bulged" mismatches destabilize the double helices by about 1.0 to 1.2 kcal/mole for the ribo-oligomers. The destabilization is about 1.8 kcal for a mismatched adenine in the deoxy-oligomers. By comparing rCA_7 + rCU_5G with rCA_6G + rCU_5G, we will see that the mismatched double helices probably form structures with dangling ends rather than bulges (see Discussion).

Ultracentrifugation of rCA_7G + rCU_7G

Ultracentrifugation equilibrium studies were carried out on the single strand oligomer rA_7G and the rCA_7G + rCU_7G double strand. The slope of a plot of log (conc) versus r^2, where r is the distance from the axis of rotation, is given by Equation (6):

$$\frac{d \log (conc)}{d r^2} = \frac{M_w(1-\bar{v}\rho)\omega^2}{4.606\ RT} \qquad (6)$$

where M_w is the weight average molecular weight (hereafter called apparent molecular weight), ω is the rotational velocity in rad/sec, $\bar{v}$ is the specific volume of the molecules, ρ is the density of the solution, R is the gas constant and T is the temperature. If the molecules do not aggregate or dissociate, the plot of log (conc) vs. r^2 should be a straight line. If there is aggregation, the slope will increase with increasing concentration.

The results of the ultracentrifugation for the single strand rA_7G in 1 M NaCl at 2°C is essentially a straight line over the concentration range of 18 μM to 490 μM, indicating that this single strand does not aggregate to a significant degree. We can thus use the molecular weight of the oligonucleotide (2742 daltons for the Na^+ salt) to obtain a value for $(1-\bar{v}\rho)$. The resulting value of 0.328, with the density of 1 M NaCl of 1.04 g/ml, yields a value of 0.646 ml/g for the specific volume of the oligomer. This specific volume corresponds to the hydrated molecule. The corresponding value for double stranded NaDNA in 1 M NaCl was measured to be 0.563 ml/g.[30] The higher value for the oligomer might be caused by a lowering of density due to a lower percentage of phosphates (there were no terminal phosphates), and to a different degree of hydration in the oligomer vs. the polymer. The buoyant density of single stranded DNA is only about 3% larger than for double strands.[31] Thus the value for $(1-\bar{v}\rho)$ determined above was used in the determination of the apparent molecular weight for the double stranded oligomer.

A plot of log (conc) vs. r^2 for the double strands $rCA_7G + rCU_7G$ is shown in Figure 3. The slope increases with increasing radius (increasing concentration), clearly indicating that aggregation is occurring. From the slopes of the curve at different values of log (conc), we can determine the apparent molecular weight as a function of concentration. The results are shown in Table VI.

DISCUSSION

It is important that we know the nature of the molecules in solution, especially since oligo-A + oligo-U form triple stranded structures in high salt concentrations.[32] Also, we want to know whether the double

helices are fraying significantly at the ends.

Several pieces of evidence indicate that the oligomers are not forming triple strands. Job plots for rCA_5G + rCU_5G in 0.05 and 1.0 M NaCl at several wavelengths show no significant concentrations of triple strands. Also, melting studies performed by mixing the strands at a ratio of 1 rCA_5G : 2 rCU_5G gave results consistent with double strand formation, even though formation of triple strands would be encouraged. Finally, NMR studies on dCA_5G + dCT_5G and rCA_5G + rCU_5G in 0.2 M NaCl indicate the absence of any significant amount of triple strand formation.[21]

The double stranded helices do not melt differentially at the ends; that is, there is not a detectable concentration of double stranded complexes in which terminal base pairs are broken. For dCA_5G + dCT_5G and rCA_5G + rCU_5G in 1.0 M NaCl, the values for $\Delta H°$ calculated by Equations (4) and (5) agree fairly well (Tables II and IV). Apparent broadening of the melting curves, due to partially melted duplexes leading to small $(df/dT)_{T_m}$ values, has been observed with oligomers such as A_nU_n, where the value of $\Delta H°$ obtained from Equation (5) is about 30% lower than that from Equation (4).[26] The fact that the two $\Delta H°$'s agree rather well in the present study might indicate that the single strand to double strand transition is essentially behaving in a two-state manner. From NMR spectroscopy on the nonexchangeable base protons, it was determined that the terminal base pairs melt at the same temperature, within experimental error, as the internal base pairs for dCA_5G + dCT_5G in 0.2 M NaCl,[21] thus further indicating the double helix melts in a two-state manner.

From statistical considerations, one would expect the terminal base pairs would not fray significantly in these oligomers, since they end in G-C base pairs. These have a greater stability constant than do A-T

(or A-U) base pairs, so at temperatures low enough to form double strands, the stability constant for the terminal base pairs is large enough to ensure completely base paired double helices.

Comparing $dCA_5G + dCT_5G$ and $rCA_5G + rCU_5G$

Table II has the thermodynamic parameters determined for $dCA_5G + dCT_5G$ in 1.0 M NaCl. The analysis was performed assuming both flat and sloping lower baselines. The values for $\Delta H°$ calculated using Equation (4) were the same within experimental error: -49 kcal/mol assuming a flat baseline, and -47 kcal/mol assuming a sloping baseline. This was true of all the oligomers in this study. The same result was found for dGCGCGC in 1.0 M NaCl.[33] The significance of a sloping lower baseline will be discussed in a later section.

The value for $\Delta H°$ calculated from the shape of the melting curve, using Equation (5), does depend on the lower baseline. Since Equation (5) assumes a two-state system, the calculation is fairly model dependent, and one would expect changing the lower baseline to affect the value of $\Delta H°$. In contrast, the calculation of $\Delta H°$ using the concentration dependence of the T_m (Equation (4)) is far less model dependent. In order to calculate the correct $\Delta H°$, you only need to select the melting temperatures such that they all correspond to the same position of the equilibrium. Thus, if the melting temperatures all corresponded to $f = 0.4$ instead of $f = 0.5$, the $\Delta H°$ calculated using Equation (4) would not be affected.

The slope of the $1/T_m$ vs. log (C_a) plot is also more accurately determined than $(df/dT)_{T_m}$. For these reasons, we use values of $\Delta H°$ determined using flat baselines and Equation (4), unless otherwise

specified. This will allow us to make direct comparisons with eariler work.

A comparison between the thermodynamics of $dCA_5G + dCT_5G$ and $rCA_5G + rCU_5G$ in 0.2 and 1.0 M NaCl are shown in Table III. The deoxy-oligomers are more stable than the ribo-oligomers. The increase in stabilization is enthalpic: -50 kcal/mol for $dCA_5G + dCT_5G$ vs. -43 kcal/mol for $rCA_5G + rCU_5G$, in 0.2 M NaCl. In the case of both deoxy- and ribo-oligomers, increasing the salt concentration from 0.2 to 1.0 M NaCl has little effect on the $\Delta H°$. The stability of both are increased somewhat, as indicated by more favorable entropies at the higher salt concentrations. The T_m's of the deoxy-oligomers increase less than the ribo-oligomers, 2.4°C and 4.7°C, respectively.

Chainlength Dependence of $rCA_nG + rCU_nG$ Thermodynamics

The thermodynamic results for $rCA_nG + rCU_nG$ for n = 5 to 7 in 1.0 M NaCl are shown in Table IV. Also included are the values predicted by Borer et al.[6]

As n becomes larger, the oligomers would be expected to behave more like $A_n + U_n$, with a larger tendency toward triple strand formation. A slope discontinuity at a ratio of 2U : 1A strands is detectable in the Job plots of $rCA_8G + rCU_8G$ in 1.0 M NaCl at low temperatures (1°C). The shapes of the melting curves of these longer oligomers were noticeably different from those for n = 5 to 7 as seen by a significant curvature in the low temperature baseline. Finally, the $\Delta H°$ calculated from the concentration dependence was anomalously high, whereas the apparent melting temperatures were too low, when compared to the shorter oligomers. As a result, $rCA_8G + rCU_8G$ and longer oligomers in this series have not been included in our analysis.

A small amount of triple helix formation in mixtures of rCA_7G + rCU_7G may be indicated by the discrepancy between the values of $\Delta H°$ calculated from Equations (4) and (5), but the amount of triple helix was too small to detect in Job plots or by increased curvature of the melting curves at low temperature.

From the chainlength dependence of the thermodynamics, we can calculate the contribution of an internal $\overset{AA}{\dot{U}\dot{U}}$ base pair to the stability of the double helix. Using the differences for n = 5 and n = 6, we obtain $\Delta H°$ (addition of $\overset{AA}{\dot{U}\dot{U}}$ base pair stack) = -9 kcal/mol, $\Delta S°$ = -28 cal/mol-°K, and $\Delta G°$ = -0.9 kcal/mol. The comparable numbers obtained by Borer et al.[6] are -8.2 kcal/mol, -24 cal/mol-°K and -1.2 kcal/mol, respectively. This agreement is reasonable, as the present study compares only two oligomers, whereas the Borer study used data for several oligomers.

From Table IV, we see that the predicted stabilities of the oligomers by Borer et al.[6] are lower than are found experimentally, although the calculations improve with increasing chainlength. The stability parameters were obtained primarily from oligomers of the type A_nXYU_n, where XY was AU, CG, or GC. As mentioned earlier, double helices with melted ends seem to contribute significantly in oligomers of the type A_nU_n. From statistical mechanical calculations, it was postulated that the terminal base pairs in A_nU_n were less stable than the internal base pairs.[34] The procedure used by Borer et al. would underestimate the stability of internal $\overset{AA}{\dot{U}\dot{U}}$ base pair stacks. This is because they essentially determine the average stability of all the $\overset{AA}{\dot{U}\dot{U}}$ stacks, and assign this value to the (more stable) internal $\overset{AA}{\dot{U}\dot{U}}$ base pairs. Since the oligomers in the present study do not terminate in A-U base pairs, the result is to underestimate the stability of these double helices.

Another possible reason for underestimation of the double helix stability is that none of the oligomers used in the Borer study contained the $\overset{CA}{GU}$ stacking interaction. They report the average stability for the $\overset{CU}{GA}$, $\overset{GA}{CU}$, and $\overset{GU}{CA}$ stacks. If the $\overset{CA}{GU}$ stack is more stable than this average value, the calculated stability will be too low.

Low Temperature Behavior of the Double Strands

The slope of the melting curves at low temperatures is surprisingly large; in fact, it is about as large as the slope of the single strand melting. Since the low temperature baselines of absorbance melting curves for polynucleotides are flat, the temperature dependence of the absorbance of oligomer double helices is thought to be an end effect. In the case of oligomers terminating in A·U base pairs, the slope can at least in part be attributed to changes in hypochromicity due to changes in the degree of base pair melting at the ends, but we do not think this occurs for the oligonucleotides studied here. It is possible that the conformation of the ends is not as rigid as it is in the interior of the double helix. Evidence supporting conformational changes comes from NMR spectra. Although the oligomers in this study are not stable enough to measure the low temperature baselines from NMR spectra, for the more stable double strands formed by dGGAATTCC, some of the base protons on each of the base pairs (including the interior ones) continue to exhibit a change in chemical shift with temperature down to 0°C.[7] We cannot say how large this change in conformation is, nor why it would occur only near the ends of double helices.

Aggregation of Double Strands

The problem of aggregation giving rise to the concentration dependent hypochromicities was presented earlier. Aggregation effects are also observed in NMR studies on dGGAATTCC,[7] and rAAGCUU,[35] as evidenced by excessive line widths of the nonexchangeable protons. The NMR spectra were run at much higher concentration (10 mM) than were used in this study.

To determine if the problem occurred optically for the single strands, the oligomers rCA_7G and rCU_7G were melted separately in 1 M NaCl over a broad concentration range. For rCA_7G, the range was from 7.9 to 720 μM; for rCU_7G, 8.7 to 800 μM. The relative melting curves superimposed over this range, indicating the effect was not occurring in the single strands. This also rules out the possibility that the effect of hypochromicities might be due to instrumental artifacts.

In an attempt to understand the nature of the double strand aggregation, we used equilibrium ultracentrifugation. This allows one to determine directly the molecular weight of a molecule, and the extent to which the molecules are aggregating.

The results of the ultracentrifugation of the single strand rA_7G shows no aggregation. The plot of log(conc) vs. r^2 was a straight line from 18 μM to 490 μM, indicating a constant apparent molecular weight vs. concentration.

The results of the ultracentrifugation for rCA_7G + rCU_7G are shown in Table IV. As can be clearly seen, the oligomers are aggregating to a significant extent over the concentration ranges commonly used for optical studies. The aggregation is significant even down to 75 μM.

The third column in Table VI shows the ratio of the apparent (weight average) molecular weight to the molecular weight calculated for the $rCA_7G + rCU_7G$ double helix. At the low concentration range, 30 μM, the ratio is 0.85. The double strand equilibrium constant at this temperature determined from the optical measurements suggest that the oligomers are greater than 99% in double strands at this concentration. Thus there is some discrepancy in the data. There are several possibilities that explain this. The errors in determining the slopes are rather large. The calculation of the apparent molecular weight is very sensitive to the value of $(1 - \bar{v}\rho)$. The value used was that obtained from rA_7G. There might be some error in this assumption, although the specific volume of double strand and single strand DNA are nearly the same. Also, degradation of the oligomer would result in a lowering of the apparent molecular weight since degradation products would contribute in such a way to lower to the apparent molecular weight. The experiment took four and a half days, so degradation is a definite possibility. The simplest model to describe the aggregation would involve assigning the same equilibrium constant, K_p, for the addition of each double strand (H) to an aggregate of n double strands:

$$H_n + H \rightleftarrows H_{n+1}$$

$$K_p = \frac{(H_{n+1})}{(H)(H_n)} \tag{7}$$

The weight average molecular weight is given by the expression:

$$M_w = \frac{\sum_{n=1}^{\infty} M_{n=1}(n^2)(S)^{n-1}}{\sum_{n=1}^{\infty} (n)(S)^{n-1}} \tag{8}$$

where $S = K_p C_t/(1 + K_p C_t)$. The resulting weight average molecular weight varies linearly with the total concentration of double helices. The best fit to the ultracentrifuge data is obtained with a value of 4200 for K_p. This corresponds to a free energy of aggregation of -4.6 kcal at 3°C. As is seen in Figure 4, the experimental data exhibit a curvature. This might be due to partial degradation of the strands, as discussed above. The model might also not be valid; the equilibrium constant may differ with the number of double helices in the aggregate.

Of course, from these data alone we cannot determine what type of aggregation is occurring. One reasonable possibility is end-to-end aggregation, where the G·C base pair of one helix stacks on that of another helix, forming a sort of double helix polymer. This could have a favorable enthalpy from the stacking interactions. It would also be accompanied by a hypochromicity, giving rise to the concentration dependent hypochromicities that we observe.

An important question is whether aggregation affects significantly the thermodynamic parameters we measure. To try to answer this, we tested a model composed of the single strand to double strand transition linked to the aggregation of double strands. The four parameters for such a model are the $\Delta H°$ and $\Delta S°$ for the double helix formation and for aggregation. The experimental parameters we fit are the melting temperatures at different concentrations.

We can simplify the model by assuming the melting curves measure directly α, the fraction of strands which are single stranded. The T_m is the temperature where $\alpha = 0.5$. We also ignore the concentration dependent hypochromicity by assigning a separate low temperature baseline for each curve.

$$\alpha = 1 - f = \frac{(A)}{C_a} \tag{9}$$

where (A) is the concentration of single strands, and C_a is the total concentration of each of the strands. Since $C_a = (A) + (H) + 2(H_2) + 3(H_3) + \ldots + n(H_n) + \ldots$, this equation can be rewritten:

$$\alpha = \frac{(A)}{(A) + (H) + 2(H_2) + 3(H_3) + \ldots + n(H_n) + \ldots} \tag{10}$$

We used a value of -4.5 kcal at 3°C for the free energy of aggregation, essentially the value determined from the ultracentrifugation. Since we do not know how to distribute this between $\Delta H°$ and $\Delta S°$, the calculations were performed by allowing the stabilization to be entirely enthalpic or entirely entropic. The results of these model calculations can then be used as a guide to determine the potential effect of the aggregation.

The fits were determined using two sets of aggregation parameters, $\Delta H°_p = -4.5$ kcal, $\Delta S°_p = 0$, and $\Delta H°_p = 0$, $\Delta S°_p = -4.5 / 276$ kcal/deg. The $\Delta H°$ and $\Delta S°$ for double helix formation were chosen to best fit the experimental T_m's. The resulting values are shown in Table VII. Calculated plots of $1/T_m$ vs. log (C_a) using both sets of $\Delta H°$ and $\Delta S°$ were essentially identical in both cases.

The effect is calculated to be quite large. Assuming the aggregation is totally enthalpy stabilized, the $\Delta H°$ for double helix formation is calculated to be -72 kcal, as compared to the value of -63 kcal in the absence of aggregation. The aggregation model tends to increase the value calculated for the double helix formation. This is because aggregation tends to increase the T_m at higher concentrations. This results in a steeper slope in the $1/T_m$ vs. log (conc) plot, and a lower $\Delta H°$. To

compensate for this, the $\Delta H°$ for double helix formation must be made larger to increase the slope back to that of the experimental curve. This result indicates that spectroscopic determinations will underestimate the $\Delta H°$ if aggregation is occurring.

The results, assuming enthalpic aggregation stabilization, are shown in Figure 5, along with the experimental T_m's. The aggregation model calculations exhibit a curvature. Since the slope of such a plot is related to the $\Delta H°$, the $\Delta H°$ for double strand formation is concentration dependent. This is an expected result, as the double strands are of course stabilized relative to the single strands when aggregates are formed. At higher concentrations, the extent of aggregation, and hence the double strand stability, increases.

There is no noticeable curvature in any of the experimental $1/T_m$ vs. log (C_a) plots we measure. The model might overestimate the effect of aggregation on the double strand formation. However, the effect of the aggregation model on the thermodynamics is large enough so that a significant effect may be present and not cause any apparent curvature in the $1/T_m$ vs. log (C_a) plots.

The extent of the effect of aggregation on the double strand thermodynamics is not apparent from spectroscopic analysis, aside from the effect of the concentration dependent hypochromicity. Unfortunately, the effect would also be difficult to detect in microcalorimetric measurements, which directly measure the amount of heat absorbed by the molecules between the low and high temperatures. This ΔH will include the contribution due to aggregation. The model presented here predicts that the amount of aggregation is large throughout the melting transition. That means the transition may be described as:

double strands (aggregated) ⇌⇌⇌⇌⇌⇌ single strands

Thus microcalorimetry will determine the sum of the enthalpic contributions. The aggregation is concentration dependent, and thus in principle the effect could be determined from the concentration dependence of the enthalpy. However, in scanning differential microcalorimetry on oligomers, the experimenters usually work at concentrations in the range of 1 mM strand concentration, and vary the concentration by a factor of about 2. Since the extent of aggregation is predicted to be large in this concentration range, the concentration effect may be too small to observe.

We have seen that the effect of aggregation on the determination of single strand to double strand energetics can be significant. A direct estimation of the extent of aggregation is obtained only from the equilibrium ultracentrifuge analysis. Thus, when studying nucleic acid oligomers at concentrations in the range of 100 to 1000 μM, care must be taken to be sure that aggregation will not significantly interfere with the results. If the aggregation is comparable in all the oligomer studies, the comparison of energetics from one set of oligomers to another set of closely related oligomers should be basically valid.

Mismatched Double Helices

A bulged structure must occur whenever a frameshift mutation occurs, and hence the stability of such a structure might be important in understanding the molecular mechanism of frameshift mutagenesis. We can form bulges by mixing oligomers with different numbers of A and U bases, for example, rCA_6G + rCU_5G. The stability of a perturbed double helix can thus be compared to that of the normal double helix.

The best estimate to date of the destabilization of a bulge is from the work of Fink and Crothers.[16] They studied poly-U + poly-(A,A*), where A* represents adenine residues modified by monoperphthalic acid to adenine-N1-oxide. By monitoring the T_m at different mole fractions of modified adenine, they were able to determine that a bulge of one nucleotide destabilizes the double helix by 2.8 kcal/mol and the triple strands by 2.3 kcal/mol. From circular dichroism measurements, they determined that the modified adenine was probably stacked in the single strand helix, but was bulged out of the double helix.[36]

We studied the thermodynamics of the mismatched double helices formed by the three mixtures: rCA_6G + rCU_5G, rCA_5G + rCU_6G, and dCA_5G + dCT_6G, in 0.2 M NaCl. The results of these studies are in Table V, along with the normal double helices for comparison. We also studied the stabilities of the mixtures rCA_7 + rCU_5G and rCA_5G + rCU_7 in order to help determine the structure of the "bulges" in the mismatched double helices. The structures of the "bulged" double helices are ambiguous. In contrast, the structure of a double helix like $rCA_7 \cdot rCU_5G$ is constrained to have a dangling end (see below).

The values for $\Delta G°$ are reported at 10°C, since the mismatched double helixes are not stable enough to study at 25°C. An extra rA or rU destabilizes the double helix by about 1.2 and 1.0 kcal/mol, respectively. The extra dT destabilizes by about 1.8 kcal/mol. In this instance, the perturbed structures are more destabilizing for dexoy-oligomers than for ribo-oligomers; however, it would be inappropriate to generalize from such limited information.

We can use the comparison between the stabilities of the double helices formed by the mixtures rCA_6G + rCU_5G with rCA_7 + rCU_5G. The possible structures for the former are represented by structures I, II,

and III in Figure 6; the most likely structure for the latter is structure IV. Equilibrium constants for each of these possible structures are defined in Figure 6.

Structures II and IV both have dangling ends containing an adenine followed by another purine, adenine or guanine. It was found that a dangling end in oligomers of the kind $A_{n+1}U_n$ stabilized the double helix relative to A_nU_n. A second dangling base, $A_{n+2}U_n$, stabilized even more, but the effect was less than the first.[26] Since the second dangling base contributes only a little, and in both structures II and IV the second dangling base is a purine, they have been assigned the same equilibrium constant, K_{d1}.

The other possible dangling end structure, III, is assigned a different equilibrium constant, K_{d2}, since it is of a different nature. The bulged structure, I, is assigned an equilibrium constant, K_b, which is an apparent equilibrium constant for all possible bulged structures. Structure I should be considered a schematic structure only. We cannot say whether the bulged base is inside the double helix or pushed out into solution. In these oligomers, there exist a number of possible sites for the bulged A. Since we do not know what the structure of the bulge is, or what the stability is at different sites, we can only assign such an apparent equilibrium constant.

The equilibrium constant for structure IV, K_{d1}, can be determined experimentally, as can be the sum of the equilibrium constants $K_b + K_{d1} + K_{d2}$. (In this case, we measure the apparent equilibrium constant for formation of all double stranded species K_{app} (double helix) = $K_b + K_{d1} + K_{d2}$.) We want to make a comparison with the corresponding normal double helix, structure V, which is assigned the equilibrium constant K_h.

The data in Table V allows us to calculate the ratio of the apparent equilibrium constants for double strand formation of the "bulged" structures (I, II and III) to the equilibrium constant for structure IV, since $\Delta G°_{app} = -RT \ln K_{app}$:

$$\frac{(K_b + K_{d1} + K_{d2})}{K_{d1}} = \frac{\exp(-\Delta G°_{app}/RT)}{\exp(-\Delta G°/RT)} = \exp((\Delta G° - \Delta G°_{app})/RT) \quad (7)$$

Table V tells us that the "bulged" structures I, II and III are more stable than the dangling end structure IV by 0.4 kcal/mol at 10°C. We estimate the error in this to be at most 0.2 kcal mol. Using the extreme value of 0.6 kcal/mol, the value of the ratio in Equation (7) is 2.9. This allows us to calculate an estimate for the lower bound for the amount of destabilization produced by a bulged adenine.

We do not know the relationship between K_{d1} and K_{d2}. If we assume $K_{d1} = K_{d2}$, then $K_b = 0.91\ K_{d1}$. This assumption is probably not strictly valid, since the stability of the dangling end probably depends on sequence. However, if we set $K_{d2} = 0.5\ K_{d1}$, the resulting free energy changes only by 0.2 kcal/mol.

Keeping in mind that 0.6 kcal/mol was an upper limit, the corresponding lower limit on the bulge destabilization can be calculated by comparing $-RT \ln (K_b)$ with $-RT \ln (K_{d1})$ and $-RT \ln (K_h)$. The last two values are directly measured. Using $K_b = 0.9\ K_{d1}$, the $\Delta G°$ for forming structure I is calculated to be -4.9 kcal/mol. Comparing these $\Delta G°$'s of double strand formation with the value for the normal double helix, -6.5 kcal/mol, the bulge destabilizes the double helix by at least 1.6 kcal/mol.

We must view these numbers with some caution, however. If we set $K_{d1} = K_{d2}$, and assume $K_b << K_{d1}$, we would expect the mixture of rCA_6G +

rCU_5G to be RT ln(2) more stable than rCA_7 + rCU_5G on the basis of statistical considerations. (The former can form dangling ends on either end; the latter on only one.) RT ln(2) = 0.39 kcal/mol at 10°C. The difference we measured was 0.4 ± 0.2 kcal/mol. Thus our data are consistent with no significant amount of bulged species, and hence the destabilizing effect of the bulge could be much greater than we just calculated. Also, since the bulge could exist in a number of places, the stability of any one of these structures would be lower than we calculate because of statistical considerations.

We also investigated the effect of an extra rU or dT base by studying the thermodynamics of rCA_5G + rCU_6G, rCA_5G + rCU_7, and dCA_5G + dCT_6G. These results are included in Table V. The possible structures for the ribo-oligomers are shown in Figure 7. In this case, we cannot follow a similar argument as above, because now the dangling end structure III' can form a G-U base pair, thus structure III' is expected to be more stable than structure II'. The difference in stability between the "bulged" structures I', II', and III' and the dangling end structure IV' should now be larger than we measured above. The observed value for a mismatched rU was 0.6 ± 0.2 kcal/mol.

In summary, we attempted to study the destabilizing effect of a bulge on double helix formation. The system we chose has the ability to form either a bulge or a dangling end. Our results indicate that the dangling end is more stable than the bulge, which indicates that a bulge destabilizes the double helix more than other perturbations. To favor the formation of a bulge, we are synthesizing molecules, for example, dCAACAAAG, which when mixed with dCT_5G should form structures with a bulged C.

Acknowledgments

This work was supported in part by National Institutes of Health Grant GM 10840 and by the Assistant Secretary for Environment, Office of Health and Environmental Research, Biomedical and Environmental Research Division of the U.S. Department of Energy under Contract No. W-7405-ENG-48.

Table I. Percent Hypochromicities and T_m's Calculated for $dCA_5G + cCT_5G$ Using Flat and Sloping Double Strand Baselines, 1 M NaCl.

	Flat Baselines		Sloping Baselines[a]	
Conc (M)	% Hypo	T_m (°C)	% Hypo	T_m (°C)
606	22	32.9	22.1	36.1
273	21	30.0	21.0	33.2
91.0	20	26.3	19.9	29.2
44.4	19.5	23.6	19.2	26.6
17.6	19	20.3	18.5	23.0
9.79	19	17.8	18.5	20.2
5.86	19	16.7	18.5	19.1

[a] Slope = 1.4×10^{-3} per °C

Table II. Thermodynamic Parameters for $dCA_5G + dCT_5G$, 1 M NaCl

	Flat Baseline		Sloping Baseline [a]	
	Conc. dep.	$(df/dT)_{T_m}$	Conc. dep.	$(df/dT)_{T_m}$
$\Delta H°$ (kcal/mol)	-49±1	-42±2	-47±2	-51±3
$\Delta S°$ (e.u.)	-145±5		-136±5	
$\Delta G°$ (kcal/mol), 25°C)	-6.1		-6.6	
T_m (200 M)	28.8		32.0	

[a] Slope = 1.4×10^{-3} per °C

Table III. Thermodynamic Parameters for $dCA_5G + dCT_5G$ and $rCA_5G + rCU_5G$ Using Flat Lower Baselines

	Conc. NaCl	ΔH° (kcal/mol)	ΔS° (e.u.)	ΔG° (kcal/mol, 25°C)	T_m (200 μM)
$dCA_5G + dCT_5G$	0.2 M[a]	-50	-149	-5.7	26.5
	1.0 M	-49	-145	-6.1	28.9
$rCA_5G + rCU_5G$	0.2 M	-43	-130	-4.6	19.2
	1.0 M	-41	-120	-5.3	23.9

[a] These values differ from those previously published (Ref. 2). An experimental error was detected and corrected.

Table IV. Thermodynamic Parameters for $rCA_nG + rCU_nG$, 1.0 M NaCl

	$\Delta H°$ (kcal/mol)		$\Delta S°$	$\Delta G°$	T_m
	Conc. dep.	$(df/dT)_{T_m}$	(e.u.)	(kcal/mol, 25°C)	(200 μM, °C)
$rCA_5G + rCU_5G$	-41	-45	-120	-5.3	23.9
calculated	-44.6		-136	-4.0	15.5
$rCA_6G + rCU_6G$	-50	-46	-148	-6.2	29.2
calculated	-52.8		-160	-5.2	23.5
$rCA_7G + rCU_7G$	-63	-53	-187	-7.3	33.8
calculated	-61.0		-183	-6.4	29.6

Table V. Effect of Mismatched Bases on Double Strand Stability, 0.2 M NaCl

	$\Delta H°$ (kcal/mol)	$\Delta G°$ (kcal/mol, 10°C)	T_m (200 μM, °C)[a]
$rCA_5G + rCU_5G$	-43	-6.5	19.2
$rCA_6G + rCU_5G$	-39	-5.3	10.8
$rCA_7 + rCU_5G$	-35	-4.9	7.7
$rCA_5G + rCU_6G$	-33	-5.5	12.9
$rCA_5G + rCU_7$	-37	-4.9	8.1
$dCA_5G + dCT_5G$	-50	-8.1	26.5
$dCA_5G + dCT_6G$	-45	-6.3	17.6

Table VI. Apparent Molecular Weight for rCA_7G + rCU_7G in 1 M NaCl.

Conc. (μM)	Apparent Molecular Weight	Degree of Polymerization*
30	5070	.85
75	8250	1.6
150	13000	2.6
410	24100	4.7
910	42900	8.5

*Apparent molecular weight divided by 5977, the molecular weight of the double helix.

Table VII. The Effect of Aggregation on Calculated Double Helix Stability for $rCA_7G + rCU_7G$.

$\Delta H^\circ_{aggreg.}$	$\Delta S^\circ_{aggreg.}$	ΔH°_{helix}	ΔS°_{helix}
kcal/mol	e.u.	kcal/mol	e.u.
0	0	-63	-187
-4.5	0	-72	-217
0	16.3	-80	-244

Figure Captions

Figure 1: Melting curves for seven concentrations of $dCA_5G + dCT_5G$ in 1 M NaCl. The absorbances were normalized to 1.0 at 50°C (see text). The concentrations and melting temperatures are listed in Table I. The upper curve is the experimental single strand melting curve.

Figure 2: The plots of $1/T_m$ vs. log (concentration) for $dCA_5G + dCT_5G$ in 1 M NaCl. ● = flat double strand baselines. ■ = sloping double strand baselines.

Figure 3: Log (concentration) vs. r^2 for the equilibrium ultracentrifugation of $rCA_7G + rCU_7G$ in 1 M NaCl at 3°C. ■ = 295 nm. ● = 290 nm. ▲ = 285 nm.

Figure 4: The plot of the ratio of the weight-average molecular weight/5977 (molecular weight of a double strand) vs. concentration for $rCA_7G + rCU_7G$ obtained from Figure 3. The straight line is the best fit for a simple aggregation model (see text), corresponding to $K_{aggreg.} = 4200$.

Figure 5: The plot of $1/T_m$ vs log (concentration) for $rCA_7G + rCU_7G$ in 1 M NaCl. ● = experimental data. —— = best fit from simple aggregation model, assuming enthalpic stabilization of the aggregation. --- = straight line fit assuming no aggregation. See Table VII for the corresponding thermodynamic values.

Figure 6: Plausible structures and equilibrium constants for the double strands formed by mixing rCA_6G + rCU_5G. Structure I should be considered as schematic only--the bulged base could be in several positions, and could be inside or outside the double helix.

Figure 7. Plausible structures and equilibrium constants for the double strands formed by mixing rCA_5G + rCU_6G.

References

1. Gilbert, W. (1976) in RNA Polymerase, Losick, R. Chamberlain, M. J., eds., pp. 195-205. Cold Spring Harbor Laboratory, New York.
2. Sims, J., Koths, K. and Dressler, D. (1978) Cold Spring Harbor Symp. Quant. Bio. 43, 349-365.
3. Schaller, H. (1978) Cold Spring Harbor Symp. Quant. Biol. 43, 401-408.
4. Huang, C. and Hearst, J. E. (1980) Analyt. Biochem. 103, 127-139.
5. Tinoco, I., Jr., Borer, P. N., Dengler, B., Levine, M. D., Uhlenbeck, O. C., Crothers, D. M. and Gralla, J. (1973) Nature New Biol. 246, 40-41.
6. Borer, P. N., Dengler, B., Tinoco, I., Jr. and Uhlenbeck, O. C. (1974) J. Mol. Biol. 86, 843-853.
7. Patel, D. J. and Canuel, L. L. (1979) J. Eur. Biochem. 96, 267-276.
8. Wells, L. R. D., Blakesley, R. W., Hardies, S. C., Horn, G. T., Larson, J. E., Selsing, E., Burd, J. F., Chan, H. W., Dodgson, J. B., Jensen, K. F., Nes, I. F. and Wartell, R. M. (1977) CRC Critical Reviews in Biochemistry 4, 305-340.
9. Haasnoot, C. A. G., den Hartog, J. H. J., de Rooij, J. F. M., van Boom, J. H. and Altona, C. (1979) Nature 281, 235-236; (1980) Nucl. Acids Res. 8, 169-181.
10. Wells, R. D., Larson, J. R., Grant, R. C., Shortle, B. R. and Cantor, C. R. (1970) J. Mol. Biol. 54, 465-497.
11. Felsenfeld, G. and Miles, H. T. (1967) Ann. Rev. Biochem. 36, 407-448.
12. Marmur, J. and Doty, P. (1962) J. Mol. Biol. 5, 109-118.
13. Lyubchenko, Y. L., Vologodskii, A. V. and Frank-Kamenetskii, M. D. (1978) Nature 271, 28-31.
14. Vizard, D. L., White, R. A. and Ansevin, A. T. (1978) Nature 275, 250-251.

15. Streisinger, G., Okada, Y., Emrich, J., Newton, J., Tsugita, A., Terzaghi, E. and Inouye, M. (1966) Cold Spring Harbor Symposium on Quantitative Biology 31, 77-84.

16. Fink, T. R. and Crothers, D. M. (1972) J. Mol. Biol. 66, 1-12.

17. Breslauer, K. J., Sturtevant, J. M. & Tinoco, I., Jr. (1975) J. Mol. Biol. 99, 549-565.

18. Adhya, S. and Gottesmann, M. (1978) Ann. Rev. Biochem. 47, 967-996.

19. Martin, F. H. & Tinoco, I., Jr. (1980) Nucl. Acids Res. 8, 2295-2300.

20. Romaniuk, P. J., Hughes, D. W., Gregoire, R. J., Bell, R. A. and Neilson, T. (1979) Biochemistry 18, 5109-5116.

21. Pardi, A., Martin, F. H. and Tinoco, I., Jr. (1980) Biochemistry, submitted.

22. Khorana, H. G. (1968) Pure Appl. Chem. 17, 349-381.

23. Goeddel, D. V., Yansura, D. G. and Caruthers, M. H. (1977) Biochemistry 16, 1765-1772.

24. Van de Sande, J. H., Caruthers, M. H., Kumar, A. and Khorana, H. G. (1976) J. Biol. Chem. 251, 571-586.

25. Fritz, H. J., Belagaje, R., Brown, E. L., Fritz, R. H., Jones, R. A. Lees, R. G. and Khorana, H. G. (1978) Biochemistry 17, 1257-1267.

26. Martin, F. H., Uhlenbeck, O. C. and Doty, P. (1971) J. Mol. Biol. 57, 201-215.

27. Uhlenbeck, O. C., Martin, F. H. and Doty, P. (1971) J. Mol. Biol. 57, 217-229.

28. Warshaw, M. M. (1965) Ph.D. Thesis, University of California, Berkeley.

29. Handbook of Biochemistry and Molecular Biology, 3rd ed., Nucleic Acids Vol. I. (1975) CRC Press, Inc. p. 589.

30. Cohen, G. and Eisenberg, H. (1968) Biopolymers 6, 1077-1100.

31. Wiesehahn, G., Cech, T. R. and Hearst, J. E. (1976) Biopolymers 15, 1591-1613.

32. Porschke, D. (1971) Biopolymers 10, 1989-2013.

33. Albergo, D. D., Marky, L. A., Breslauer, K. J. and Turner, D. H. (1980) Biochemistry, submitted.

34. Levine, M. D. (1974) Ph.D. Thesis, University of California, Berkeley.

35. Borer, P. N., Kan, L. S. and Ts'o, P. O. P. (1975) Biochemistry 14, 4847-4863.

36. Fink, T. R. and Crothers (1972) Biopolymers 11, 127-136.

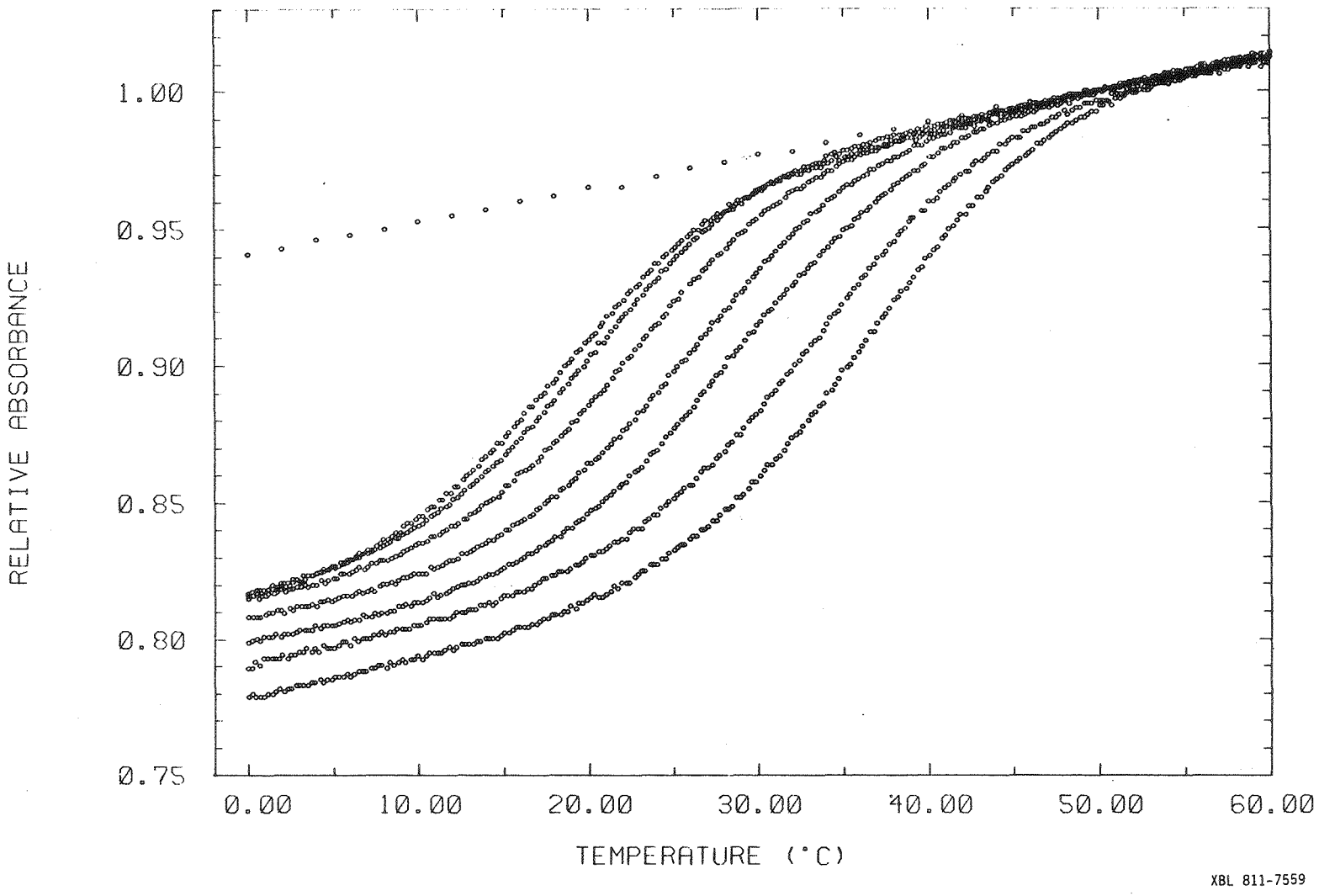
RELATIVE ABSORBANCE
1.00
0.95
0.90
0.85
0.80
0.75
0.00
10.00
20.00
30.00
40.00
50.00
60.00
TEMPERATURE (°C)
XBL 811-7559

Figure 1.

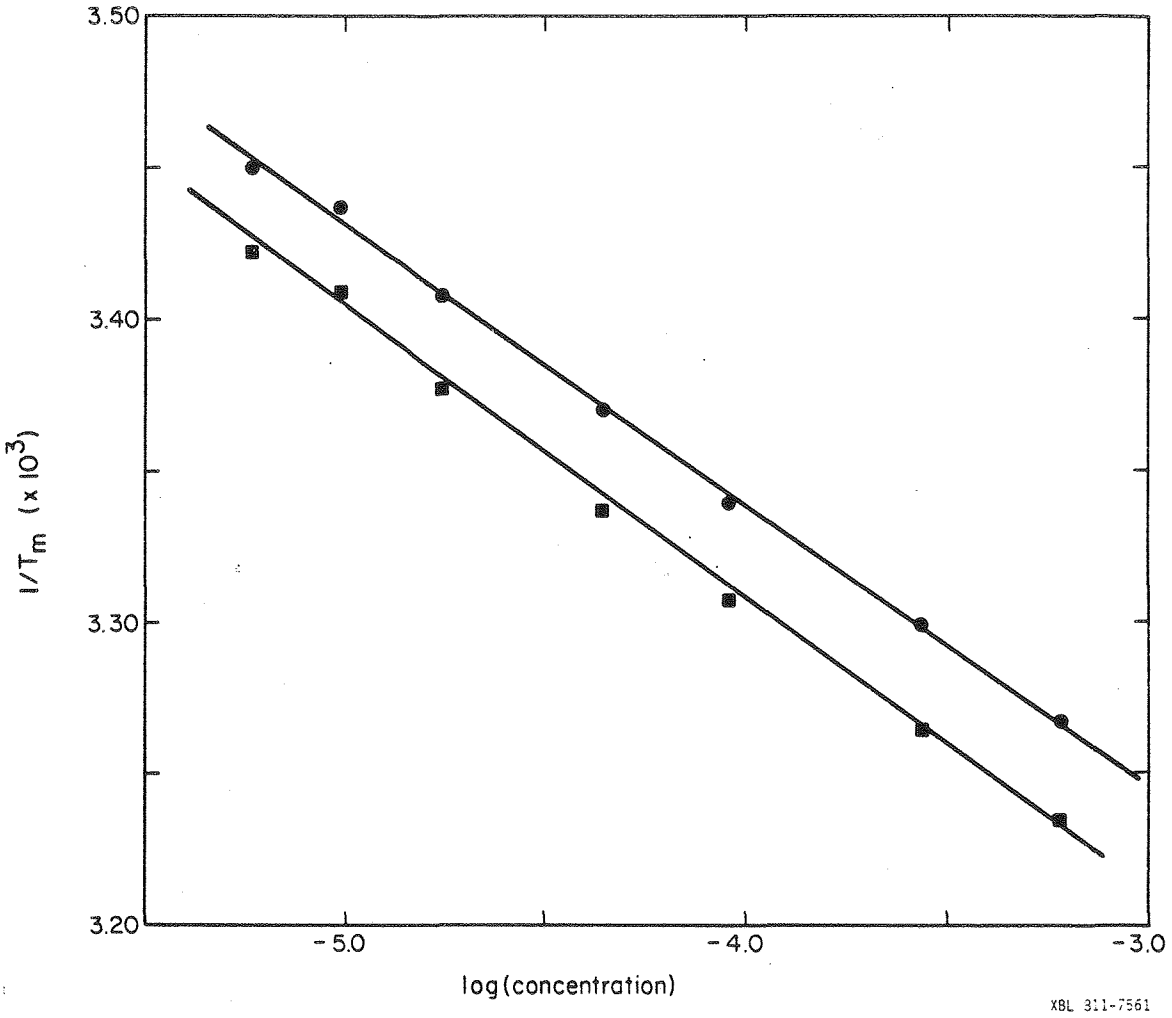
3.50
3.40
3.30
3.20
$1/T_m$ ($\times 10^3$)
-5.0
-4.0
-3.0
log(concentration)
XBL 811-7561

Figure 2

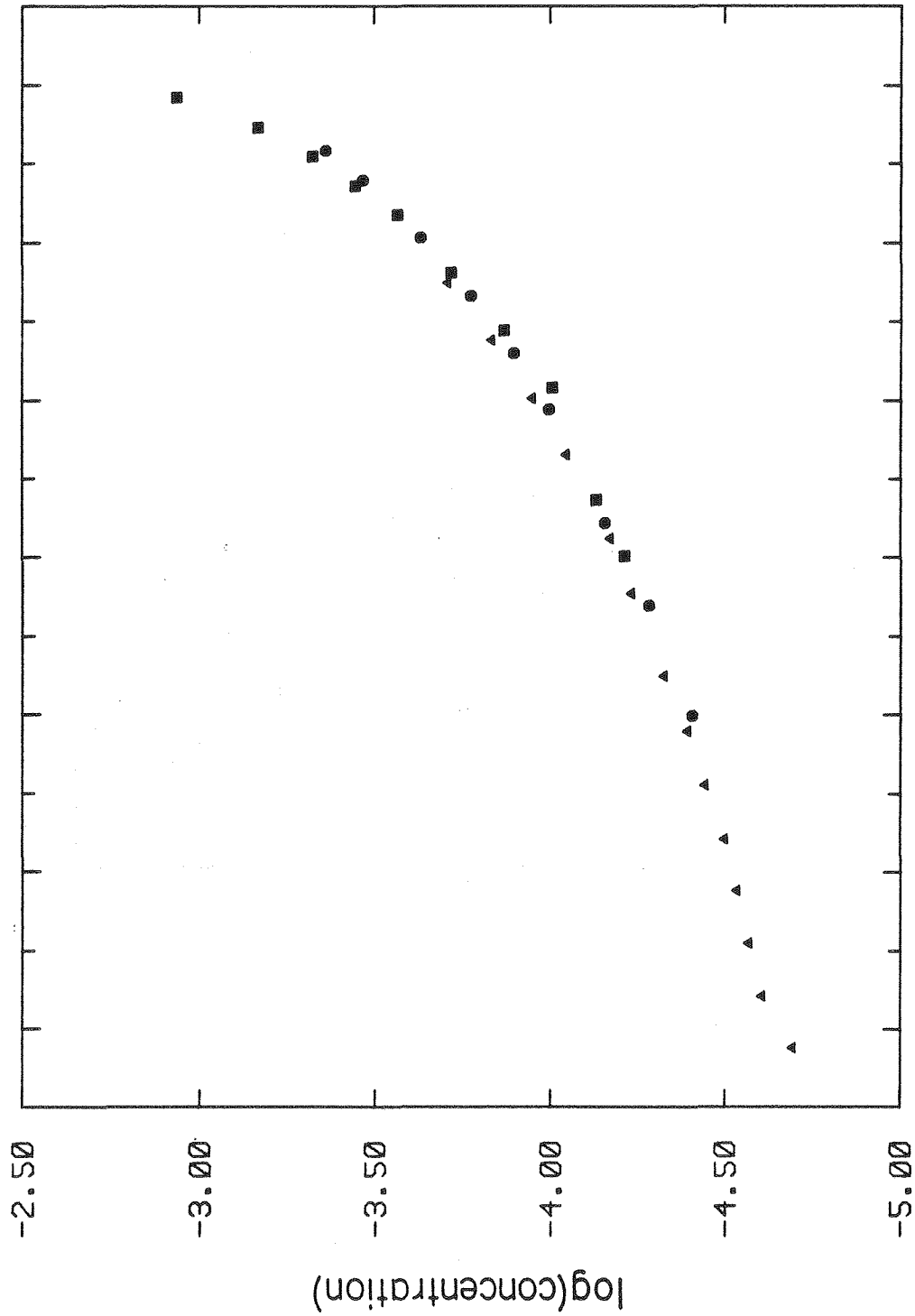

XBL 811-7562

Figure 3

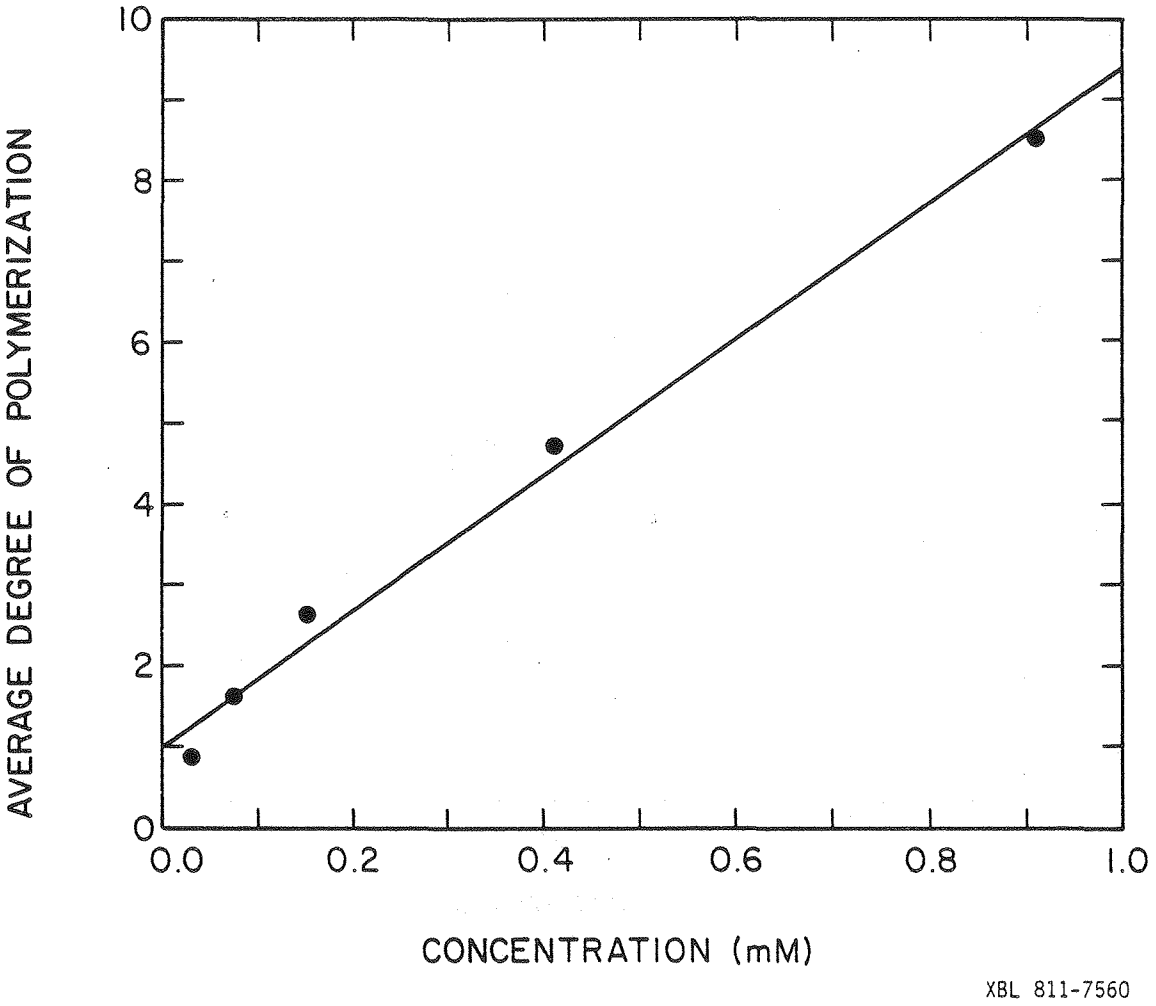
AVERAGE DEGREE OF POLYMERIZATION
0
2
4
6
8
10
0.0
0.2
0.4
0.6
0.8
1.0
CONCENTRATION (mM)
XBL 811-7560

Figure 4

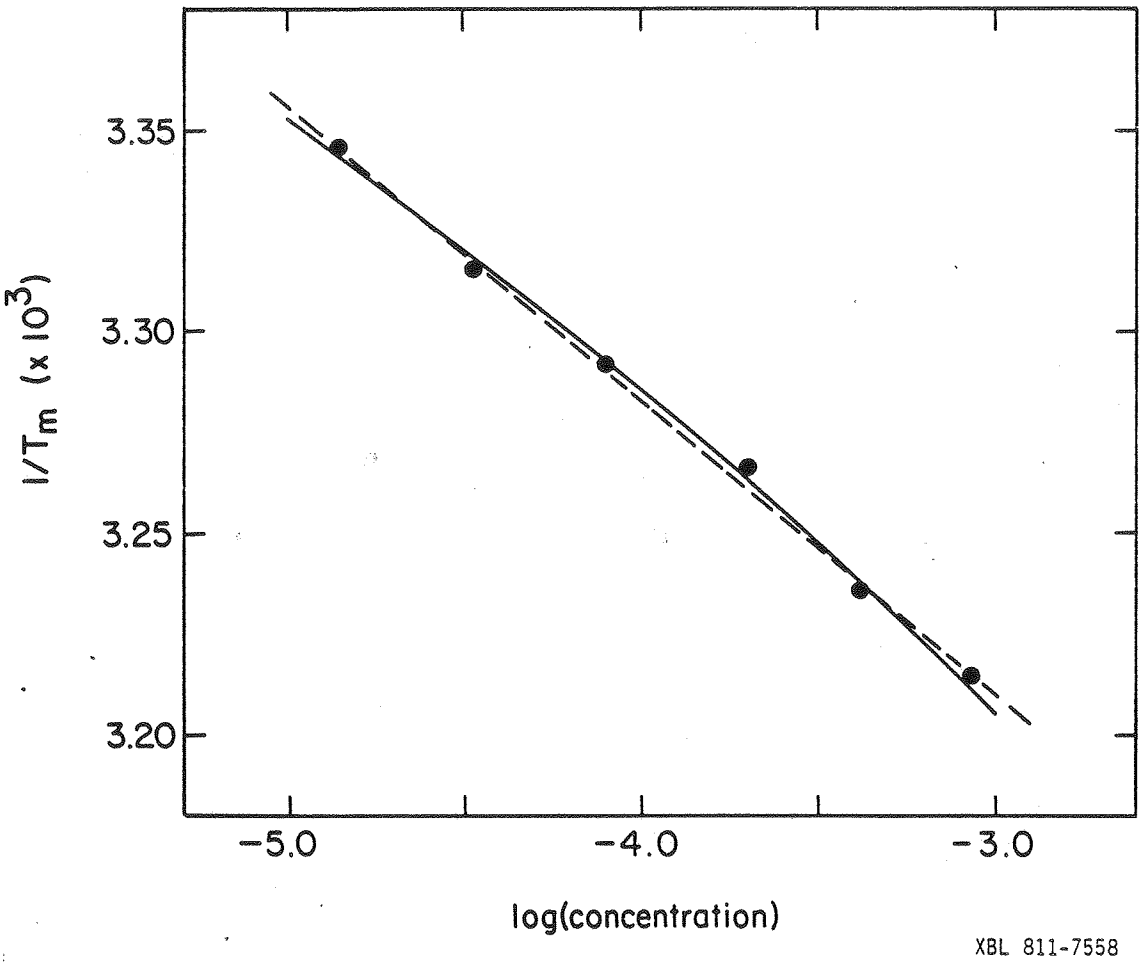
3.35
3.30
3.25
3.20
$1/T_m$ ($\times 10^3$)
-5.0
-4.0
-3.0
log(concentration)
XBL 811-7558

Figure 5

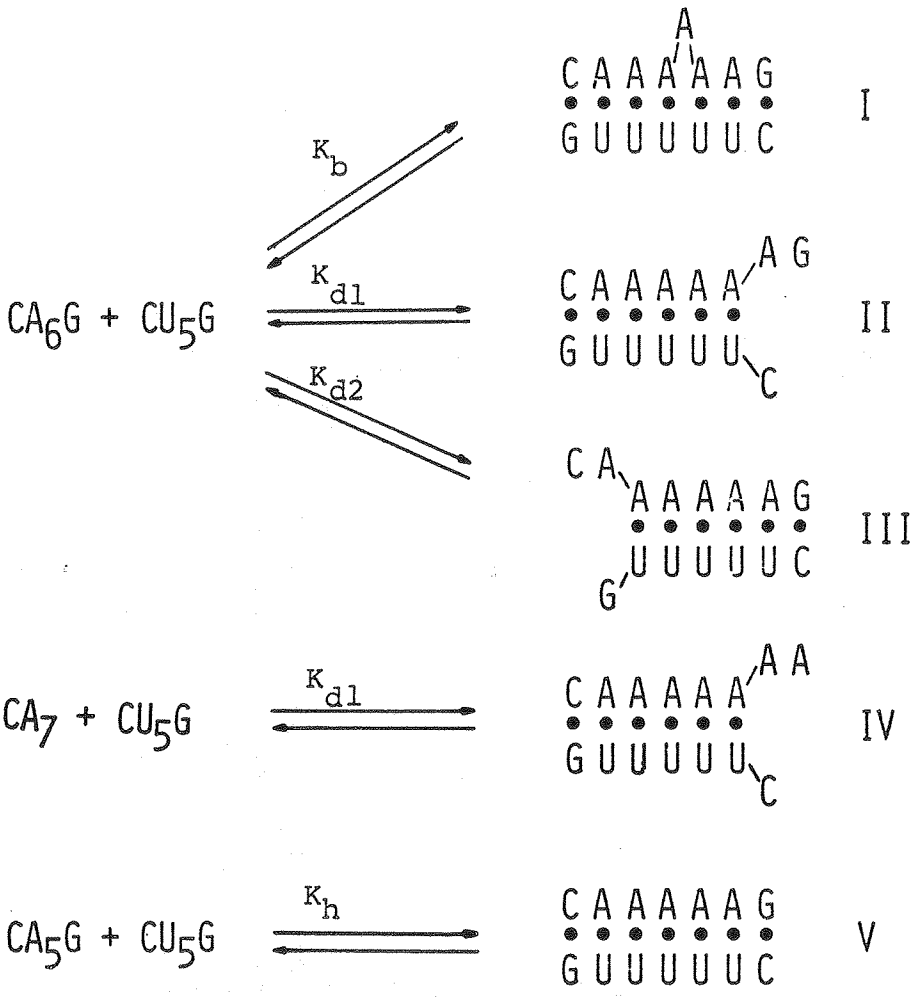

Figure 6

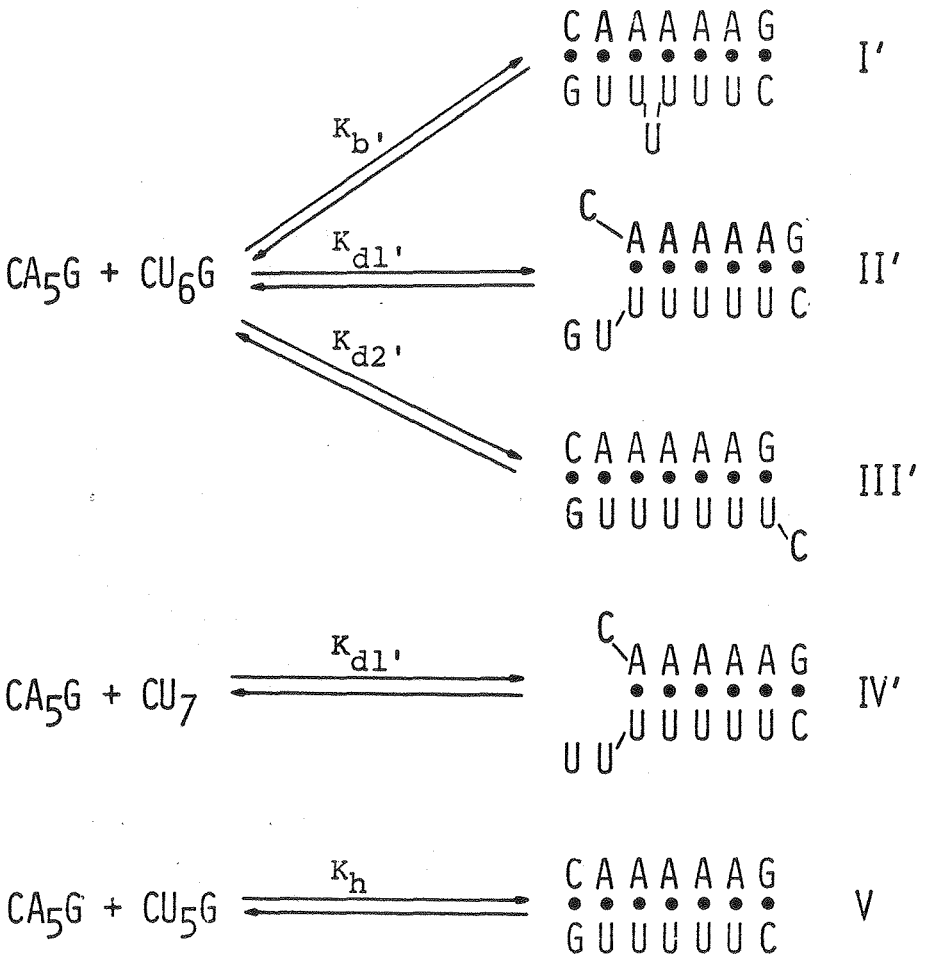

Figure 7